A Mathematical Model of a Packed-Bed Heat-Exchanger Reactor For Dehydrogenation of Methylcyclohexane: Comparison of Predictions with Experimental Results

R. D. HAWTHORN, G. H. ACKERMAN, and A. C. NIXON

Shell Development Company, Emeryville, California

The selective, highly endothermic reaction of methylcyclohexane to toluene and hydrogen was studied experimentally over a commercial Pt/Al_2O_3 catalyst, in an electrically heated tube serving as a packed-bed reactor heat exchanger. The constant-flux reactor, with measurement of temperatures within the bed at points intermediate along its length, proved well suited as an integral reactor for providing information on the reaction rate. A simple analytical model of the reactor was developed, and some of the data were used with the model to derive a rate expression.

The model gives a good representation of radial variation of temperature in the packed bed. In the region of high Reynolds numbers investigated, radial transport of enthalpy is described in the model by a film resistance at the tube wall defined by heat transfer coefficient, and a diffusive transport through the packing, dominated by eddy diffusion.

In a packed-bed reactor, in which heat is supplied or removed through the wall of the reactor tube (a heat-exchanger reactor), radial gradients of temperature and, to a lesser extent, of concentration develop within the reactor. In addition, of course, concentration and temperature also vary in the direction of flow, the axial direction. The description of even the steady state behavior of such a reactor requires taking into account these variations in both directions and their influences on local values of the rates of chemical reactions within the reactor tube. Such gradients in concentration and temperature result primarily from interaction between the chemical reaction rate and the radial and axial transport processes within the reactor. These transport processes in packed beds have been studied extensively as separate phenomena. As a result of such studies, at least empirical representations of these processes are available. The integration of this information with chemical reaction-rate expressions to formulate mathematical models to describe the behavior of packed-bed reactors has been a subject of considerable interest to chemical engineers in recent years. As a result, formal models for such descriptions have been developed in considerable detail (*2, 4*). However, empirical evaluations of the ability of such models to represent the results of experiments in packed catalytic reactors have received less attention in the literature. This paper will

present a comparison of experimental results obtained for a particular highly endothermic reaction, the dehydrogenation of methylcyclohexane to toluene, with the predictions of a relatively simple model developed in a conventional manner for this reaction.

The experimental program and the development of a model for the reaction system to allow extrapolation of experimental results were practically motivated by a rather unusual application of heat-exchanger reactors. They are part of an overall program carried out under U.S. Air Force sponsorship to evaluate the potential of hydrocarbons to serve not only as fuel but also as coolant in high-speed aircraft (Mach 3-12). In such a speed range the convention coolant, air, is no longer available for this use because of its high stagnation temperature. As an alternative fluid to absorb internal heat loads, the fuel is a logical possibility. In such a system the heat absorbed by the fuel is ultimately rejected from the aircraft as sensible heat in the combustion products, the combustion temperature being higher because the fuel absorbed heat before being burned. In the range of aircraft speeds of interest, the total heat load to be absorbed by the coolant (increasingly a function of aircraft speed) is beyond the capability of a hydrocarbon to accommodate as latent and sensible heat and still remain below the temperature at which thermal decomposition reactions would rapidly lead to coking and fouling of the heat-exchange system. To obtain additional heat-absorbing capacity, hydrocarbons which can undergo highly endothermic reactions have been considered. Furthermore, to allow such reactions to be carried out at reasonable temperatures and with high selectivity, thus enabling maximum utility to be obtained from the endothermicity of the reaction, catalysis of such reactions is being studied.

The most promising class of reactions studied is the dehydrogenation of naphthenes to aromatics, typified by the reaction of methylcyclohexane (MCH) to form toluene and hydrogen, the reaction studied in the work reported here. The experiments, in view of their ultimate applications, were aimed at studying the heat-exchange properties of the reacting system. Therefore, the heat-exchanger reactor was viewed primarily as a heat exchanger in planning the experimental program. An additional bias on the conditions selected for the experiments, imposed by their intended application, is that the conditions studied were those associated with a high throughput per unit volume or weight. Indeed, the range of Reynolds number studied extends to considerably higher values than those customarily covered in studies of packed beds.

In the present study, the heat-exchanger reactor was idealized as a single, cylindrical tube packed with catalyst and heated uniformly over its surface. Reactants flow

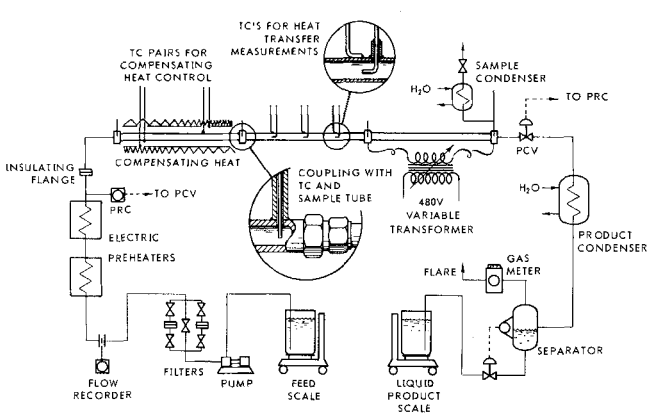

Fig. 1. Flow sketch of fuel system simulation test rig.

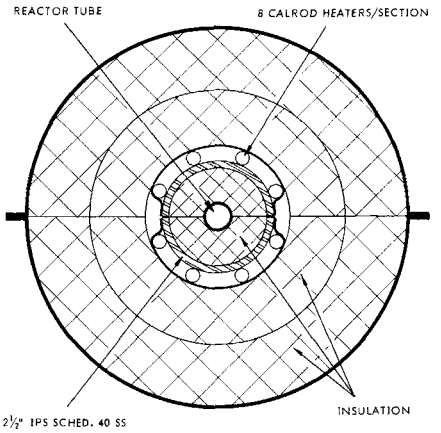

Fig. 2. FSSTR-cross section sketch.

axially through the tube, their reaction being catalyzed by active sites within the porous packing. Because of the geometrical symmetry of the bed and the uniform heating rate around the periphery of the tube it was presumed that radial profiles of all variables would be axisymmetric. No specific experimental verification of this assumption was undertaken.

EXPERIMENTAL PROCEDURE

Equipment

The test unit used in obtaining the data reported here was assembled for the purpose of determining the heat-sink capabilities of various hydrocarbon fuels which might be used in high-speed aircraft.

The system, a flow sketch of which is given in Figure 1, consists of a feed tank, positive displacement pump, filters, flow recorder, preheaters, three 10 ft.-long reactor sections, pressure control valve, product condenser, and liquid product receiver and gas metering and vent system. The operating limits of the unit are 16 gal./hr. at 1,000 lb/sq.in. gauge, preheat temperature 800°F., reactor temperature 1,500°F.

The reactor sections used for thermal-reaction studies are ⅜-in. O.D. by 0.049-in.-wall Hastelloy C tubing. For catalytic reactions one of these sections may be filled with catalyst, or a ¾-in. O.D. by 0.049-in.-wall Hastelloy C tube may be substituted for one of the small diameter sections.

The tubes are individually resistance-heated by the output of variable transformers capable of supplying 13 kw. to the ⅜-in. O.D. or 25 kw. to the ¾-in. O.D. sections. To make the system adiabatic, the tubes are insulated and surrounded by compensating heaters. These Calrod heaters are specially wound to provide a linearly varying power density along their length. Eight of these heaters are mounted around a shell (2.5 in. IPS schedule-40 stainless steel pipe) which encloses each length of the test section. By installing adjacent heaters with their power gradients in opposite directions and controlling the two sets separately, one can maintain the shell at any desired linear temperature profile to approximate the test-section profile. Figure 2, a cross section of a reactor section, illustrates the compensating heat-insulation assembly around the reactor tube.

As shown in the insets of Figure 1, three tube-wall and fluid thermocouple pairs are provided for heat-transfer measurement in each reactor section. Fluid temperatures are also determined at the ends of each section. A typical temperature profile for the reactor system when heat is being added in each section and an endothermic reaction is taking place in Section II is illustrated in Figure 3.

Two measurements of energy input to the reactor were available for each run: from direct measurement of electrical power input and from an overall heat balance on the fluid entering and leaving the reactor. The difference between these two, about 7% for experiments in the smaller tube and

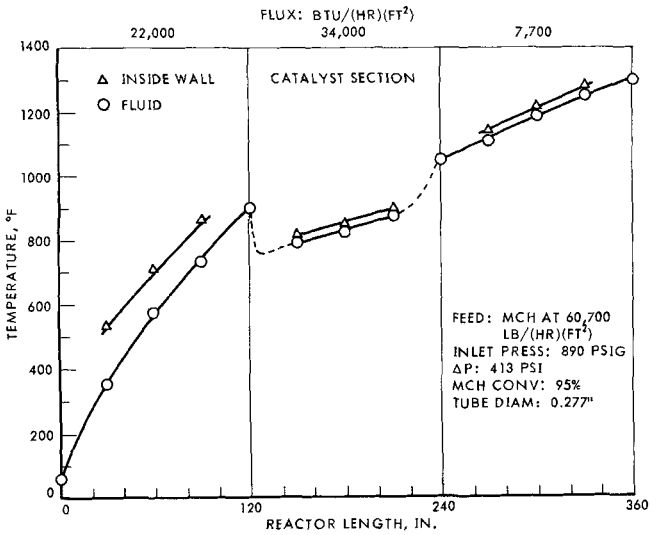

Fig. 3. Typical temperature profile.

about 3% for those in the larger tube, probably resulted from a combination of heat losses and inaccuracies in the measurement of electrical power input. In subsequent analysis and comparison with calculations of the reactor model, the power input derived from the heat balance on the fluid was used preferentially for experiments in the smaller tube.

Since the tube-wall thermocouples were welded to the outside surface of the tube and the heat was being transferred from the inside surface which was at a lower temperature, a correction was applied to the measured temperatures to give the ΔT values tabulated in the summary tables and used in calculation of heat-transfer coefficients. This correction was calculated from the following equation:

$$\Delta T_W = \frac{q/A}{2\,k_w}\,m \qquad (1)$$

Procedure

For a test run with this equipment, the following procedure was used. MCH feed was started, and the desired flow rate and system inlet pressure were established. Power was supplied to the appropriate reactor sections and slowly increased until the desired operating temperatures were reached. At the same time, power was started to the compensating Calrod heaters and the control was activated to maintain 0° temperature differential between reactor tube and guard-heat tube at the two control points. When steady state conditions had been maintained for at least 20 min., data, other than temperatures, were recorded and final product samples were taken. Temperatures were recorded by multipoint instruments throughout the operating period. As the recorders used for temperature monitoring had 0 to 1800°F. charts, reading temperature differentials to <2°F. was questionable, and therefore all runs where the calculated temperature drop across the fluid film at the reactor wall was less than 10°F. have been excluded in analysis of heat transfer. Operating data for all tests included in this study are incorporated in the summary tabulations, Tables 1 and 2.*

Both ⅜-in. O.D. by 0.049-in.-wall and ¾-in. O.D. by 0.049-in.-wall reactor tubes were used in this investigation. In both cases the catalyst charge was 1/16-in. spheres of UOP-R8 platinum on alumina. A single charge of catalyst was used for each tube size during these runs. Before initial use each charge was activated in situ by being maintained at 1,050 to 1,100°F. for 1 to 2 hr. with nitrogen flowing through the reactor. Between operating periods the reactor was flushed with nitrogen and allowed to cool. The operating conditions covered in this study represent an unusual application for this commercial reforming catalyst (*6*). The reactor feed in all cases was pure hydrocarbon, with no additional hydrogen supplied. Thus, the only hydrogen present in the reactor was that generated by the dehydrogenation reaction. In addition, reactor temperatures in these experiments extended to a maximum of 1,050°F., considerably higher than the customary operating temperature for this catalyst. Although no explicit study of catalyst life was undertaken here, the two catalyst charges used were subjected respectively to over 4,000 volumes (as liquid) of feed/volume of catalyst and over 1,000 volumes of feed/volume of catalyst under a variety of operating conditions, without apparent deactivation.

Within the range of conditions studied, the catalyst used promotes a highly selective conversion of MCH to toluene. In rather complete analysis of reactor products by gas chromatography and mass spectrometry, the only products of side reactions found in significant amounts were dimethyl and ethyl cyclopentanes. These were found in minor quantities, generally less than 1%*m.* of the hydrocarbon. While this side reaction was taken into account in the original analysis of the data and in the modeling of the reactor, it has been omitted in reporting the results here in order to simplify the presentation. Minor amounts of methylcyclohexadienes and dealkylation products were also found. However, quantities of these products were so small that it was not necessary to take the reactions producing them into account for our purposes. Test conditions covered approximately the following ranges

Feed rate:	17,000-70,000 lb./(hr.)(sq.ft.)
Pressure (inlet):	500-900 lb./sq.in.gauge
Fluid temp. (T_o):	690-890°F.
Heat flux (q/A)	12,000-51,000 B.t.u./(hr.)(sq.ft.)

Each experiment, carried out at a fixed inlet pressure and temperature, reactant flow rate, and heat flux, provided values at three axial locations along the reactor of the tube-wall temperature and the temperature of the fluid at the center line of the reactor. (These were in addition to an average conversion, fluid temperature, and pressure at the reactor outlet also provided by the experiment.) Viewed as temperature differences, these pairs of temperatures provided information on the radial temperature profiles within the reactor. However, because the heat input to the fluid over any portion of the reactor was specified by the experimental conditions, the fluid temperatures measured at intermediate points also contributed information on the extent of chemical reaction which had taken place upstream of each of these three points. Data were obtained from experiments under twelve sets of experimental conditions in the smaller tube (two of which were fourfold replicate experiments) and from seven sets of experimental conditions in the larger diameter tube.

During the course of the study of the catalytic dehydrogenation reaction, heat transfer data were also obtained on unpacked ⅜-in O.D. reactor sections. While not tabulated in this paper, these data serve as an indication of the suitability of the test unit for heat transfer measurements.

For the empty-tube condition, three general categories of data were included: (1) those from section I of the apparatus serving as a preheater for pure MCH, (2) those from section III selving to heat products of reaction (primarily toluene/$3H_2$), and (3) some results from thermal cracking runs in which both product and reactant were present and reaction was taking place. In all cases the system pressure was above the critical pressure for the working fluid. However, in the case of the data obtained in section I the temperature was low enough so that the MCH was in a liquidlike fluid state.

Figure 4 shows a comparison of the experimental data for the MCH system with the Dittus-Boelter correlation:

$$N_{Nu} = 0.023\,N_{Re}^{0.8}N_{Pr}^{0.4} \qquad (2)$$

The data show some scatter but quite good agreement with this correlation, with a best-fit correlation line of this form being given by the Dittus-Boelter correlation. No significant

* Tabular material has been deposited as document 9710 with the American Documentation Institute, Photoduplication Service, Library of Congress, Washington 25, D. C., and may be obtained for $1.25 for photoprints or 35-mm. microfilm.

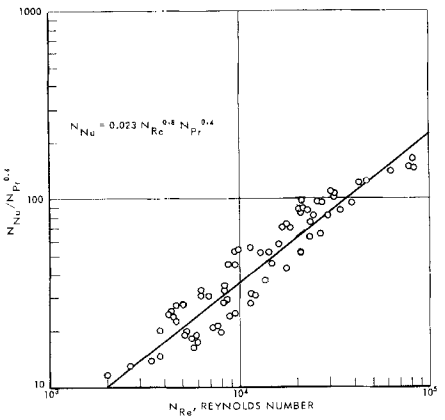

Fig. 4. Correlation for heat transfer coefficients to MCH in empty tube.

discrepancies were noted between the three categories of data used in this comparison.

DEVELOPMENT OF MODEL FOR THE REACTOR

The pattern followed in developing a continuum model for a cylindrical, packed-bed reactor was that described in detail by Beek (2), with the additional simplifying assumption that any radial variation in mass velocity of the fluid could be neglected. The basic assumptions made are then: (1) the flow is axially symmetric and the mass velocity is uniform over the cross section, (2) axial diffusion and conduction may be neglected, and, (3) molecular diffusion may be neglected. The last assumption is particularly important. By imposing the same (eddy) diffusivity on all chemical species, the material balance may be written in terms of conversion rather than concentration of each component.

With these assumptions the steady state equations for material and energy transport are

$$\frac{\partial x}{\partial z} = \frac{4d_p}{r_t^2 N_{Pe}}\left(u\frac{\partial^2 x}{\partial u^2} + \frac{\partial x}{\partial u}\right) + \frac{R}{G} \tag{3}$$

and

$$\frac{\partial T}{\partial z} = \frac{4d_p}{r_t^2 N_{Pe}}\left(u\frac{\partial^2 T}{\partial u^2} + \frac{\partial T}{\partial u}\right) + \frac{4k}{GC_p r_t^2}\left[u\frac{\partial^2 T}{\partial u^2} + \left(1 + \frac{u}{k}\frac{\partial k}{\partial u}\right)\frac{\partial T}{\partial u}\right] + \frac{4d_p}{r_t^2 N_{Pe}}\left[2\left(\frac{\partial C_p}{\partial x}\right)\left(\frac{\partial x}{\partial u}\right) + \left(\frac{\partial C_p}{\partial T}\right)\left(\frac{\partial T}{\partial u}\right)\right] \frac{u}{C_p}\left(\frac{\partial T}{\partial u}\right) - \frac{RQ}{GC_p} \tag{4}$$

In both equations, the radial variable is expressed as

$$u = \left(\frac{r}{r_t}\right)^2$$

which is the form used in subsequent numerical treatment of the equations. The material-transport equation employs the conversion x as the dependent variable. In writing the enthalpy-transport equation the radial diffusivity for heat is assumed to be the sum of an eddy diffusivity, contained in the Peclet number, and a noneddy diffusivity, k, the latter being related to the transport of heat via conduction through the fluid, conduction through the packing, and radiation. In subsequent numerical treatment of the enthalpy balance it is convenient to lump all the terms on the right-hand side, except the first, together into a source term since components of these terms vary axially as well as radially. Thus, the two equations may be written in simplified comparable form:

$$\dot{x} = \omega\,(ux'' + x') + S_m \tag{5}$$

$$\dot{T} = \omega\,(uT'' + T') + S_h \tag{6}$$

The boundary conditions at the tube wall ($u = 1$) are

$$x' = \frac{\partial x}{\partial u} = 0 \tag{7}$$

and

$$T' = \frac{\partial T}{\partial u} = -\frac{(r_t\, h_w\,(T - T_w)}{2\left(\dfrac{GC_p d_p}{N_{Pe}} + k\right)} \tag{8a}$$

$$T' = \frac{\partial T}{\partial u} = \frac{q/A \cdot r_t}{2\left(\dfrac{G\,C_p d_p}{N_{Pe}} + k\right)} \tag{8b}$$

In simulating experiments in the present program, the temperature boundary condition was used in the form of Equation (8*b*), since the heat flux was the specified quantity. Therefore, h_w, the heat transfer coefficient at the wall, was not necessary for calculation of the performance of the packed bed but only to relate the measured wall temperature to temperatures within the packing. To calculate the wall temperature, T_w, for these experimental conditions, the equivalence of Equations (8*a*) and (8*b*) was used. For numerical solution, the boundary conditions at the tube center line need not be stated explicitly since they are taken into account in the form of the equations.

In order to use these equations it is necessary to be able to supply values for all of the parameters appearing in them as functions of the two dependent and two independent variables. On the basis of existing knowledge of processes in packed beds and of transport and thermodynamic properties of fluids, this is possible without experimental study of the particular reaction system for all of the parameters except those actually entering into the determination of the chemical reaction rate.

The following representations of these parameters were used in model calculations in this study.

The Peclet number, assumed to be constant throughout the reactor and the same for mass as for enthalpy transport was taken to have a value of 10.0. All of the model calculations and all of the experiments being simulated were clearly in the turbulent flow regime, with Reynolds numbers, based on particle diameter, of greater than 10^3. The total thermal conductivity was treated by the method suggested by Beek (2):

$$\text{Koverall} = \underbrace{\frac{C_p G d_p}{N_{Pe}}}_{\text{eddy}} + \underbrace{\frac{0.6\, h_p\, d_p\, k_s}{2k_s + 0.7\, h_p d_p}}_{\text{packing}} + \underbrace{2\,\sigma' r\, d_p\, T^3}_{\text{radiation}} \tag{9}$$

The present investigation did not provide a critical test of this expression since, at the high mass velocities studied, the eddy portion of the conductivity dominated the remaining contributions very strongly.

The heat capacity of each component was assumed to be of the form

$$(C_p)_k = a_k + b_k\,(T - T_R) \tag{10}$$

Zero-pressure heat capacities tabulated in API 44 (1) were used in determining these linear coefficients. The

molar heat capacity of the mixture was assumed to be linear in the mole fractions of components. The heat of reaction was also taken from the low-pressure value calculated from the values given in API 44 (*1*) tables at the reference temperature, T_R, and assumed to vary with temperature in a manner consistent with the assumed linear variation of heat capacities with temperature.

The heat transfer coefficient from the fluid to the catalyst particles is that suggested by Beek (*2*) for spherical particles:

$$h_p = \frac{k_f}{d_p}\left[3.22\,N_{Re}^{1/3}N_{Pr}^{1/3} + 0.117\,N_{Re}^{0.8}N_{Pr}^{0.4}\right] \quad (11)$$

The heat transfer coefficient at the wall is given by

$$h_w = \frac{k_f}{d_p}\left[0.28\,N_{Re}^{0.77}\,N_{Pr}^{0.4}\right] \quad (12)$$

In these expressions the Reynolds number is defined as

$$N_{Re} = \frac{d_p G}{\mu_f}$$

The expression for the coefficient at the wall is substantially that given by Hanratty (*5*) for transfer to beds packed with spherical particles, with the constant adjusted for the definition of Reynolds number used here and for the inclusion of the influence of Prandtl number.

Transport properties of the fluid, k_f, μ_f, and N_{Pr}, were calculated from correlations as functions of temperature, pressure, and composition. For use in the computer calculations based on the model, a constant set of values was used for each run throughout the calculation. These values were calculated for a set of average conditions within the reactor. For subsequent comparisons of measured and calculated temperature differences local values of these properties were also calculated. The predicted heat transfer coefficients and temperature differences were not very sensitive to the conditions used in calculating viscosity and thermal conductivity since these properties vary together with pressure, temperature, and composition and appear as nearly a ratio in the heat transfer coefficient correlations.

The variation of pressure within the bed, while it does not appear explicitly in the transport equations, is involved in the analysis because of its effect on the rate of chemical reactions. The differential equation used for pressure drop is

$$\dot{P} = \frac{\partial P}{\partial z} = \bar{f}\frac{G^2}{g_c \rho d_p}\cdot A_f \quad (13)$$

where A_f is an empirical factor allowing for the influence of the ratio of the tube diameter to the particle diameter (d_t/d_p) on the pressure gradient. It was necessary to use experimental data from reactor runs to evaluate this factor for each of the tube sizes used. Best fits with the two groups of experimental data were obtained with values of A_f of 0.5 for $d_t/d_p = 4.4$ and of 0.67 for $d_t/d_p = 10.4$. For the friction factor, the correlation given by Ergun (3) was used:

$$\bar{f} = \frac{1-\epsilon}{\epsilon^3}\left(1.75 + 150\frac{1-\epsilon}{N_{Re}}\right) \quad (14)$$

Thus, except for the single empirical factor in the pressure-drop expression and except for an expression relating the rate of the chemical reaction to local concentrations and temperature, the model description of the packed-bed reactor is constructed of correlations, parameter values, and assumptions available before any experiments were carried out in the reactor system used here.

REACTION KINETICS

The data obtained under the twelve sets of conditions for which experiments were carried out in the smaller-diameter tube were used in developing and testing reaction-rate expressions and in evaluating parameters in these expressions. The rate expression, when used in conjunction with the remainder of the packed-reactor model, was required to reproduce not only the outlet temperature and conversion, but also the axial profile of the temperature along the reactor center line, which had been measured experimentally for each set of conditions. Taking a pragmatic rather than a mechanistic attitude toward developing a satisfactory rate expression, we searched for the simplest relationship which could satisfy the experimentally measured criteria. In attempting to develop this expression, we allowed for heat transfer between the gas phase and the catalyst-pellet surface but took no explicit account of mass transfer outside the pellet or of either diffusion or heat transfer within the pellet. Thus, the rate expression was used to relate gas-phase compositions and the temperature of the pellet surface, T_s, to the reaction rate. The surface temperature is related to the gas-phase temperature, T_g, by the equation

$$T_s = T_g + \frac{R\,\Delta H\,d_p}{6h_p} \quad (15)$$

Information from previous studies of this reaction over similar catalysts indicated that the reaction rate far from equilibrium was independent of hydrogen and toluene concentration and depended upon MCH concentration less strongly than did first order reactions. Attempts to fit experimental temperature profiles with a simple rate expression, reversible and first order in MCH concentration, were unsuccessful. Such a rate expression generated an axial temperature profile considerably steeper than the experimental one in the region of low conversion (up to about 50%). Quite satisfactory results were obtained ultimately with the form proposed by Sinfelt (*7, 8*) for this reaction over a similar Pt/Al_2O_3 catalyst, simply modified to allow for reversibility of the reaction:

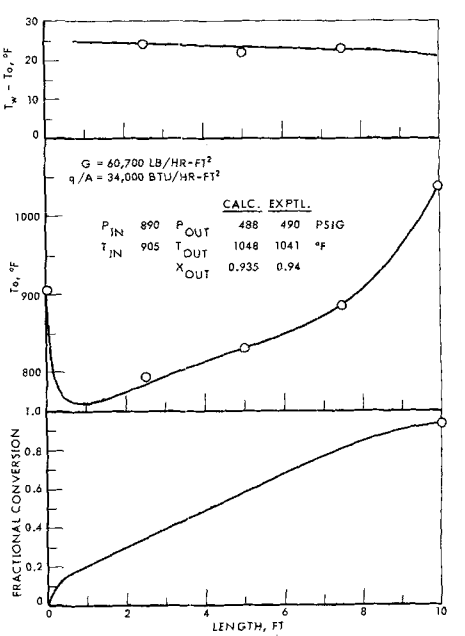

Fig. 5. Calculated axial profiles of conversion and temperature for high mass velocity in the smaller tube.

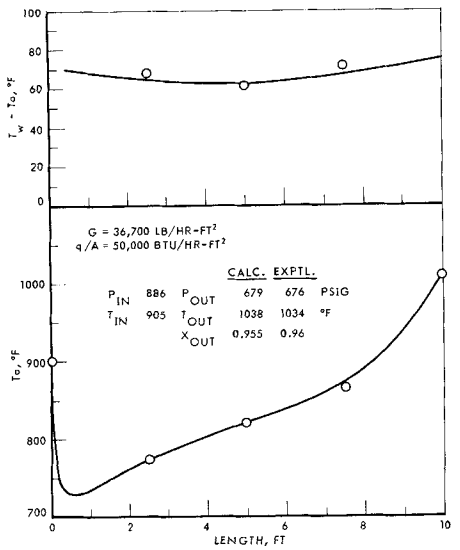

Fig. 6. Calculated axial profiles of temperature for high mass velocity in the larger tube.

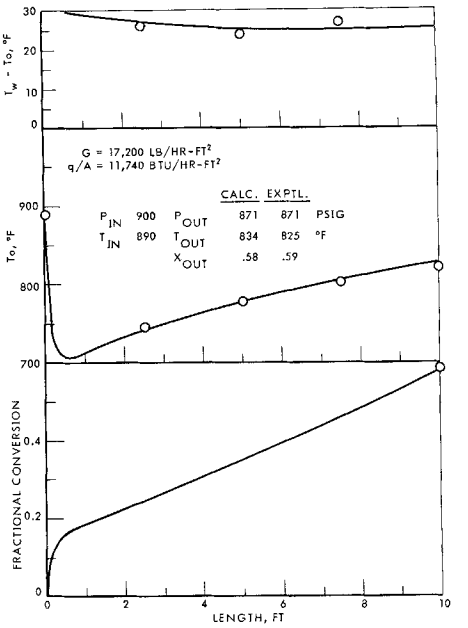

Fig. 7. Calculated axial profiles of temperature and conversion for low mass velocity in the larger tube.

$$R = \frac{(1-\epsilon)\, A_1\, C_{MCH} \exp\left(\frac{B_1}{R_g T_s}\right)}{1 + A_2\, C_{MCH} \exp\left(\frac{B_2}{R_g T_s}\right)} \left[1 - \frac{P_{Tol}\, P_{H_2}{}^3}{P_{MCH}\, K_{eq}}\right] \tag{16}$$

where the parameters have the values

$A_1 = 100$ sec.$^{-1}$
$A_2 = 2.8 \times 10^{-6}$ cc./g.-mole
$B_1 = -3.0$ Kcal./g.-mole
$B_2 = +30.0$ Kcal./g.-mole

Comparisons of the data for a representative experiment with the results of calculations for these conditions using the packed-reactor model with the above rate expression and constants are shown in Figure 5. Similar comparisons of experimental and calculated results for the entire set of runs are given in Table 1.* Of particular significance is the comparison of experimentally measured temperatures on the center line of the reactor (represented by the open points) with the calculated axial profile of centerline temperature (given by the curve). It can be seen from this figure that the model calculations give a very close approximation of the experimental axial temperature profiles. For the entire set of experimental data obtained in the smaller-diameter tube the root-mean-square discrepancy between calculated and experimental temperatures is slightly less than 6°F.

The lower curves in Figures 5 and 7 are calculated axial profiles of average conversion. They illustrate the behavior of a reactor with constant heat input along its length. At the inlet end, because the feed was overheated when brought into the reactor, the conversion rises rapidly as the fluid temperature falls to a level where the rate of the endothermic reaction is just able to accommodate the rate of heat input. Through most of the remainder of the reactor, the average rate of reaction remains nearly constant, with the fluid temperature rising to compensate for the decrease in reactant concentration in order to maintain a constant rate. In this region nearly all (over 80%) of the added heat is taken up by the endothermic reaction. In the run illustrated in Figure 5, near the outlet end a high rate of conversion could no longer be sustained owing to reactant exhaustion as equilibrium conditions were approached. In this region, temperature increased rapidly as a progressively increasing fraction of the heat input was accommodated as sensible heat by the fluid.

* See footnote on page 71.

NUMERICAL TREATMENT OF THE MODEL

The numerical method used in solution of the partial differential equations for material and enthalpy transport [Equations (5) to (8)] is a simple, explicit scheme. Axial derivatives are represented by forward-difference approximations, radial derivatives at all points, including the boundaries, by three-point approximations with a truncation error of the order of the square of the radial step size. The source terms are evaluated on the known (n^{th}) profile. A separate one-dimensional forward-difference equation was used for calculating the pressure.

With this explicit forward-difference system, for the high-aspect ratios (L/d_t) of the reactors studied here, accuracy requirements could be imposed only in the selection of the number of radial increments. The corresponding axial step size required for stability of the numerical solution was always very much less than required for reasonable accuracy in the axial direction. Even in the selection of the radial increment, little advantage in accuracy was found by using more than two radial increments (the minimum number for which the scheme can be used). Increasing the number of radial increments from two to four changed the calculated radial temperature difference (between wall and center line) by less than 0.4°F. out of a total of 65°F. and the value of the center line temperature by less than 0.1°F. for the most demanding conditions (highest heat flux, larger tube diameter).

PREDICTION OF CONVERSION AND AXIAL TEMPERATURE PROFILES

Of the data obtained in the set of experiments in the smaller-diameter tube, only the measured radial temperature differences were not used in developing the model and establishing its free parameters. The results of experiments in the larger-diameter tube constitute a distinct set of data. These seven experiments were carried out in a

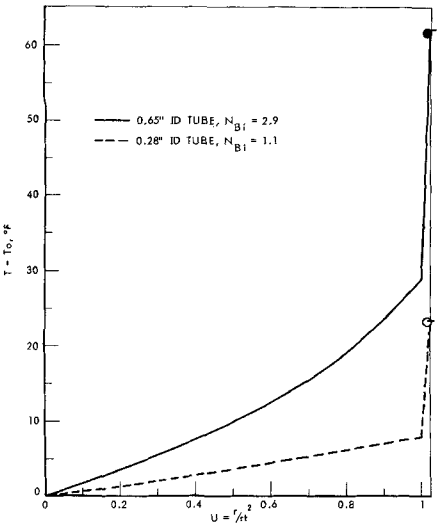

Fig. 8. Calculated radial temperature profiles at axial midpoint of tube.

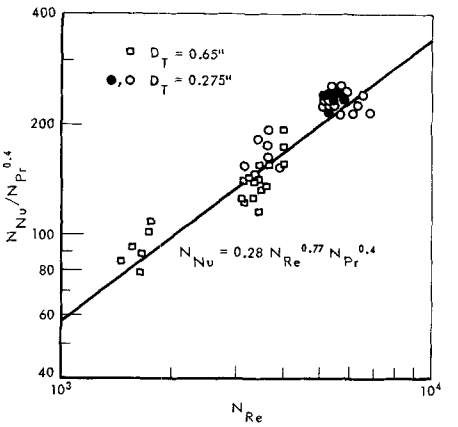

Fig. 9. Experimentally derived coefficients of heat transfer at tube wall compared with correlation.

different though overlapping range of mass velocities with a different charge of catalyst but, most important, in a tube of large enough diameter that radial gradients of temperature within the packed bed became a significant factor in determining the reactor performance. Except for the pressure drops measured in this set of experiments all the data obtained in them are available for independent evaluation of the capabilities of the model.

Calculations from the model are compared in Table 2* with experimental results for data obtained in the larger-diameter tube. Examples of this comparison are shown for two sets of conditions in Figures 6 and 7, where the points represent experimental measurements and the curves represent the results of calculations. In a comparison of temperatures on the axial profile at the reactor center line, the root-mean-square discrepancy is 6.5°F. for the entire set. This is only slightly larger than the discrepancy observed with the data from the smaller tube.

RADIAL TEMPERATURE DIFFERENCES

Experimentally the quantity measured was effectively the difference in temperature between the inside of the reactor tube wall and the center line of the packed bed. In the model this temperature difference is considered as composed of two parts, a temperature difference across a fictive-film heat transfer resistance at the wall and a temperature difference through the packing, determined by an effective diffusivity. The two curves shown on Figure 8 illustrate the division of this temperature difference into these two components and compare the total calculated value with the experimental measurements for these two particular conditions. For the lower (dotted) curve, which represents the radial profile for the axial midpoint of the reactor in an experiment in the smaller-diameter tube, the total temperature difference (both measured and calculated) was 23°F. Of this, 15°F., nearly two-thirds of the total, is accounted for by the film resistance at the wall; the temperature variation through the packing is only 8°F. Because of the small radial temperature variation through the packing, the reaction rate was nearly uniform over the cross section and the temperature profile is nearly parabolic in radius. Such an experiment could well be described by a one-dimensional model, using the parabolic approximation for the radial temperature profile to relate the measured center line and wall temperatures to the average fluid temperature at which the rate is calculated in such a model. For the upper (solid) curve representing an experiment in the larger tube, the total temperature difference is 62°F., with 33°F. across the film and 29°F. through the packing. Here the temperature variation through the packing is great enough to influence the reaction rate significantly. As a result, the radial temperature profile is much flatter than parabolic. For this experiment, one-dimensional modeling would be less successful.

The upper portions of Figures 5 through 7 show comparisons of the measured values of the temperature difference between center line and tube wall with axial profiles of this temperature difference calculated using the model described above. Discrepancies between experimental and calculated values are within the range of expected experimental error, 4°F. max.

Figure 9 presents an alternative method of evaluating the ability of the model to represent radial temperature differences. From the experimental measurement of the total radial temperature difference, the portion calculated (by the model) to occur across the packing was subtracted, leaving a portion attributable to the wall-film resistance. This portion was used together with the experimental heat flux to calculate the coefficient of heat transfer at the wall and a corresponding Nusselt number. The Nusselt number calculated in this manner is compared as a point in Figure 9 with the correlation incorporated in the model for the calculation of this heat transfer coefficient. Solid points shown represent the average from fourfold replicate runs; open points represent single experiments. Although the experimentally based points in this figure show considerable scatter, they are well represented by the correlation line, with a maximum deviation under 25% and a root-mean-square deviation of about 10%. The correlation shown in Figure 9 is based on that derived by Hanratty (5) from the data of Plautz, which covered a range of Reynolds numbers (as defined here) up to about 1,800. The data obtained in this investigation provide justification for the use of this correlation at significantly higher Reynolds numbers, up to at least 7,000.

The comparisons given in Figures 5 through 7 and Figure 9 show that the model described here gives a good representation of the overall radial temperature differences measured in the experimental program. In view of the range of conditions of the experiments, the representation by the model can be said to be confirmed only in the range of highly turbulent flow through the packed bed of spherical particles. In this range the model for radial transport of enthalpy consists essentially of a film resistance at the wall, described by a heat transfer coefficient given by Equation (12) in series with diffusive transport through

* See footnote on page 71.

the packing, with an effective conductivity corresponding to a radial Peclet number of 10.

RADIAL VARIATION OF CONCENTRATION

Calculations with the model gave the expected result; that radial variation of composition was small under all conditions studied. The maximum variation in conversion between wall and center line was 1.5%. With a reaction rate depending on reactant concentration less strongly than first order, such small variations in concentration have only a minor influence in making the reaction rate nonuniform over the reaction cross section. Such nonuniformity of reaction rate is due almost entirely to radial variation of temperature.

SUMMARY

The selective, highly endothermic reaction of methylcyclohexane to toluene and hydrogen was studied experimentally over a commercial Pt/Al_2O_3 catalyst. The experimental studies were carried out in an electrically heated tube serving as a packed-bed reactor heat exchanger with a uniform heat flux imposed over the tube surface. Experiments were concentrated in a region of mass velocity higher than normally used in packed-bed reactors. The simple analytical model of the packed-bed reactor that was developed is capable of simulating the experimental results and is suitable for extrapolation to conditions outside the range studied. The constant-flux reactor, with temperatures within the packed bed measured at points intermediate along its length, proved well suited as an integral reactor for providing information on the rate of reaction. Some of the experimental data were used together with the developed model to derive a useful rate expression for the reaction/catalyst combination. This rate expression is given by Equation (16).

The model of the packed-bed reactor developed in this investigation gives a good representation of radial variation of temperature in the packed bed, at least in the range of high Reynolds numbers for which experiments were made. In this region radial transport of enthalpy is described in the model by a film resistance at the tube wall defined by the heat transfer coefficient given by Equation (12), and a diffusive transport through the packing, dominated by eddy diffusion with a diffusivity derived from a value of 10.0 for the Peclet number.

ACKNOWLEDGMENT

We are indebted to our colleagues J. Beek, Jr., and A. M. Benson, who earlier developed a computational program for packed-bed reactors which served as a pattern for the one used in this study, for their advice and interest and to R. E. Taber for assistance in the laboratory. The catalyst used in the experimental study was supplied by Universal Oil Products.

This work was done under the sponsorship of the Fuels, Lubricants, and Hazards Branch of the Air Force Aero-Propulsion Laboratory, Wright-Patterson Air Force Base with H. Lander as the Project Engineer. Permission to publish from the Air Force and Shell Development Company is gratefully acknowledged.

NOTATION

a_k = constant in linear expression for heat capacity of species k
A_1, A_2 = kinetic constants, preexponential factors
A_f = wall effect factor in pressure drop equation
b_k = constant in linear expression for heat capacity of species k
B_1, B_2 = kinetic constants, temperature coefficients
C_p = heat capacity
C_{MCH} = concentration of MCH
d_p = particle diameter
d_t = tube diameter
$\bar{f}$ = friction factor
G = mass velocity
g_c = gravitational conversion factor
ΔH = enthalpy change in reaction
h_p = heat transfer coefficient, fluid to particle
h_w = heat transfer coefficient, wall to packed bed
h = heat transfer coefficient
k = noneddy part of effective radial thermal conductivity of packed bed
k_{eff} = effective thermal conductivity (radial) of packed bed
k_f = thermal conductivity of fluid
k_s = thermal conductivity of solid pellets of catalyst
k_w = thermal conductivity of tube wall
K_{eq} = equilibrium constant for reaction
L = reactor length
m = wall thickness of reactor tube
N_{Bi} = Biot number, $h_w r_t/k_{eff}$
N_{Nu} = Nusselt number, $h_w d_p/k_f$
N_{Pe} = Peclet number, Gd_p/D_r (where D_r is the radial diffusivity for mass) or $C_p G d_p/(k_{eff} - k)$
N_{Pr} = Prandtl number, $C_p\mu_f/k_f$
N_{Re} = Reynolds number, $d_p G/\mu_f$
P = pressure
P_i = partial pressure of i^{th} component
q/A = heat flux
Q = heat of reaction, $-\Delta H$
r = radius, position variable
r_t = tube radius
R = reaction rate
R_g = gas constant
S_h = source term in enthalpy equation
S_m = source term in material equation
T = temperature
T_o = fluid temperature at reactor center line
T_g = fluid temperature
T_w = temperature of inside wall of reactor tube
T_s = temperature of catalyst pellet
T_R = reference temperature
ΔT_w = temperature difference through metal tube wall
u = $(r/r_t)^2$, dimensionless radial variable
x = conversion
z = axial variable

Greek Letters

ϵ = fraction voids
μ_f = viscosity of fluid
ρ = density of fluid
σ_r' = effective radiation constant
ω = coefficient in P.D.E. for material and enthalpy transport

LITERATURE CITED

1. *American Petroleum Institute Research Project 44,* New York.
2. Beek, J., Jr., in "Advances in Chemical Engineering," Vol. 3, pp. 203-271, Academic Press, New York (1962).
3. Ergun, S., *Chem. Eng. Progr.*, **48**, 89 (1952).
4. Froment, G. F., *Ind. Eng. Chem.*, **59**, No. 2, 18 (1967).
5. Hanratty, T. J., *Chem. Eng. Sci.*, **3**, 209 (1954).
6. Ritchie, A. W., and A. C. Nixon, *Ind. Eng. Chem. Prod. Res. Develop.*, **5**, 59 (1966).
7. Sinfelt, J. H., in "Advances in Chemical Engineering," Vol. 5, pp. 50-55, Academic Press, New York (1964).
8. Sinfelt, J. H., H. Hurwitz, and R. A. Shulman, *J. Phys. Chem.*, **64**, 1559 (1960).

Manuscript received June 22, 1967; revision received October 19, 1967; paper accepted October 20, 1967.